Dynamics of polymer knots at equilibrium

Pik-Yin Lai*
Department of Physics and Center for Complex Systems, National Central University, Chung-li, Taiwan 320, Republic of China
(Received 3 January 2002; published 26 August 2002)

The relaxation and diffusion dynamics of knotted polymers at equilibrium under good solvent conditions are investigated by dynamic Monte Carlo simulations. Prime knots of chain lengths up to $N=240$ monomers and knots up to 20 essential crossings are studied. The relaxation dynamics of the prime knots at equilibrium do not display the classification into group as in the case of the nonequilibrium relaxation of cut knots [Phys. Rev. E **58**, R1222 (1998); Phys. Rev. Lett. **87**, 175503 (2001)]. Furthermore, the time autocorrelation functions for the radius of gyration of the nontrivial knots can be fitted by a sum of two exponential decays of long and short characteristic relaxation times. These two relaxation times decrease with the number of essential crossings C. The faster relaxation follows the Rouse behavior and scales as $N^{1+2\nu}$ and its dependence on C is consistent with the scaling analysis using the blob picture. The mean-square displacement of the center of mass of the knots obeys the free diffusion behavior compatible with the Rouse dynamics. The diffusion coefficients of the knots, $D\sim 1/N$ for large N, but D decreases for knots with increasing C. These results are analyzed using scaling theories and discussed in terms of topological interactions in the knots.

DOI: 10.1103/PhysRevE.66.021805 PACS number(s): 61.41.+e, 47.50.+d, 87.10.+e

I. INTRODUCTION

Recent advances in single-molecule experimental techniques in chemical and biological systems enable the direct manipulation of naturally occurring knotted DNA [1–4] as well as artificially tying up a molecule into a knot [5]. Also, Type II topoisomerases can affect the global topology of ring DNA [6,7] and the reaction rate is believed to be governed by the intrinsic relaxation dynamics of the knotted DNA. It urges for some fundamental understanding of the physical and dynamical properties of knotted chain molecules. On the other hand, the breakthrough of Jones polynomials [8] in knot theory, has boosted much research interest in the connection between physics and knot theory, especially on spin models in statistical mechanics [9,10] for the last decade. Also, there have been some advances in the emergence of knotlike structures in quantum and classical field theories recently [11,12]. Even then, the connection tends to be mathematical and abstract, still far from direct physical observations. It is clear that the topological constraint in a knotted molecule dictates the important physical and geometrical properties of the knot [13–22]. In a similar way, the entanglement effects in a dense polymer melt give rise to the topological interactions that govern the dynamics in polymeric systems. The constraint of no chain crossing and no chain breaking in a knot restricts the number of possible conformations that can only appear or disappear via continuous chain deformations. Topological interactions are easy to picture but hard to quantify, yet they are robust and have good memories, even prehistoric men used knots as mnemonic devices to record events and numbers before the invention of symbols/words. These topological interactions are manifested most prominently in knots, and knotted polymers are convenient systems for studying them. The fact that closed ring polymers possess topological memory is expected to hinder their relaxation motions. It is interesting to probe such pure topological effects and clarify its effects on the dynamical properties of knotted molecules. However, in real experiments, these topological interactions often mix up with other interactions such as energetic interaction among monomers and solvent or the intrinsic bond energies or chemical properties of the ring molecule. Thus it is desirable to investigate the dynamics of knotted polymers in a computer simulation, which is dominated by the topological interactions.

Our previous study on the *nonequilibrium* relaxation times of prime knots revealed that knots are naturally classified into group according to their characteristic times to untie when the well-equilibrated knot is cut. The Alexander polynomials of the knots within a group can be parametrized in the same way [17,18]. It is of interest to see whether such classification will emerge in the dynamical properties of these knots at thermal equilibrium. Using dynamic Monte Carlo simulations, we consider knots formed by flexible polymers in good solvent conditions. Only excluded volume effects and the topological constraint of no segment crossing are present in our systems. Topological effects are expected to dominate in the dynamical properties in knots. Previous scaling prediction for the dependence of the relaxation times on the essential crossing number (C) of the knot was not satisfactorily verified in the simulation data in Ref. [16]. In this paper, we reexamine the relaxation times of the knots, especially focusing on its dependence on C, by simulation and scaling calculations. Various ring polymers as listed explicitly in Table I are studied. Section II gives some basics about knots and describes the bond-fluctuation model and simulation details. The simulation results for the autocorrelation functions and diffusion dynamics are presented in Sec. III. The data of the equilibrium relaxation times and diffusion constants are discussed by scaling analysis in terms of the blob picture and inflated tube model, respectively. Finally, Sec. V gives some outlook and discussions.

*Email address: pylai@phy.ncu.edu.tw

TABLE I. Values of the exponents α of various prime knots.

Knot C_K	α
3_1	2.01 ± 0.08
4_1	2.37 ± 0.1
5_1	2.27 ± 0.1
5_2	2.26 ± 0.2
6_1	2.58 ± 0.1

II. MODEL AND SIMULATION DETAILS

The conventional nomenclature of a knot is denoted by C_K where C is the number of essential crossings [26] in any planar projection, i.e., the minimum number of crossings no matter how one tries to untie the knot without cutting it, and K is just a label to distinguish topologically different knots. Two knots are topologically the same if they can be transformed into each other with only three kinds of Reidemeister moves [26]. Prime knots up to ten essential crossings were listed by Tait and Little [27,28] in the 19th century. Prime knots are knots that are not composed of simpler knots. Traditionally, knots are just simply arranged in an increasing order of C in usual knot tables or knot diagrams. C is a fairly weak topological invariant and can have an exponentially large degeneracy when C is large. For instance, there are seven knots with seven crossings and 9988 knots with 13 crossings. Advances had been made in classifying knots and topological invariants [8–10]. More sophisticated topological invariants such as Alexander, Jones polynomials, and Vassiliev invariant can distinguish knots much better, but there is still no one-to-one correspondence for more complex knots. For instance, 5_1 and 10_{132} have the same Alexander polynomial. The search for an ultimate invariant for a one-to-one classification of all the knots remains one of the fundamental challenges in mathematical knot theory. The equilibrium dynamics of three knot groups (see Fig. 1), namely, the torus knots $(3_1,5_1,7_1,\ldots)$, the even twist knots $(4_1,6_1,8_1,\ldots)$ and the odd twist knots $(5_2,7_2,9_2,\ldots)$ are investigated in this work. These knots have been shown to classify into the above three groups in terms of their nonequilibrium relaxation times [17,18]. The numbering of the prime knots in this study follows that of Alexander and Briggs [29] for knot up to $C=9$ and from Conway [30] for knots with $C=10$. For $C \geqslant 11$, a straightforward generalization in each knot group is used.

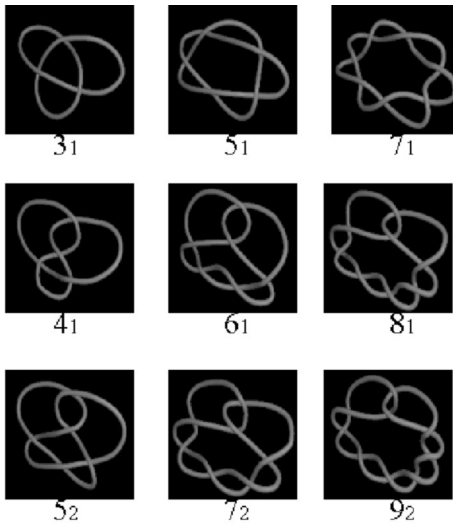

FIG. 1. Knot diagrams for various knot groups in this study. The torus knots $(3_1,5_1,7_1,\ldots)$, the even twist knots $(4_1,6_1,8_1,\ldots)$, and the odd twist knots $(5_2,7_2,9_2,\ldots)$.

The bond fluctuation model (BFM) for macromolecular chains [23] is employed for the polymer knots. The BFM for polymer chains in three dimensions [24] is a coarse-grained lattice model in which each effective monomer occupies a cube of eight sites in a simple cubic lattice. A polymer chain is represented by a sequence of successive monomers linked by effective bonds taken from a set of 108 allowed bond vectors from the set of all permutations obtained by symmetry operations of the cubic lattice: $\{P(2,0,0), P(2,1,0), P(2,1,1), P(2,2,1), P(3,0,0), P(3,1,0)\}$. Here, $P(2,0,0)$ denotes all the possible permutations of the bond vectors generated from (2,0,0), which include the six bond vectors $(\pm 2,0,0)$, $(0,\pm 2,0)$, and $(0,0,\pm 2)$. The bond lengths in the BFM can range from 2 to $\sqrt{10}$ in units of lattice spacing. Hard-core self-avoiding interaction between monomers is imposed by the requirement that no two monomers can share a common site. The dynamics of this model are introduced by choosing a monomer at random and attempting to move it by one lattice spacing in one of six randomly selected directions: $\pm x$, $\pm y$, $\pm z$. This move attempt will be accepted if the following conditions are satisfied: (1) self-avoidance is obeyed; (2) the new bond vector still belongs to the allowed set. Because of the requirement that the bonds must stay in the allowed set, no two bonds will ever intersect each other in the course of the motion; hence, the entanglement effect is taken care of automatically. Because of its more realistic and simple moves, this model is suitable for the study of dynamical properties of polymers. Also, it has been established that this model is in agreement with the Rouse model in the dilute limit or with the reptation model for long chains in entangled melts [25] in three dimensions. The polymer chain in the BFM has a wide spectrum of bond angles and bond lengths as compared with conventional lattice polymer models. It has many features of an off-lattice model but at the same time has the advantage of lying on a lattice in which a fast computing algorithm can be implemented. Solvent molecules hit the monomers due to thermal motion and give rise to solvent viscosity and this effect is modeled as the random Monte Carlo trials moves of the monomers. It is well established that polymers give rise to entropic elasticity [31] and the topological contraint and entanglement in the knot restrict its conformation and hence affect the global stiffness of the knot.

A single ring polymer chain consists of N monomers is placed inside a cubic box with periodic boundary conditions imposed in all three directions. There are only two basic interactions in our model: the first is the excluded volume effects between the monomers which can be thought of as a knot having a finite cross-section thickness; the second being the prohibition of any segment crossing in the course of the

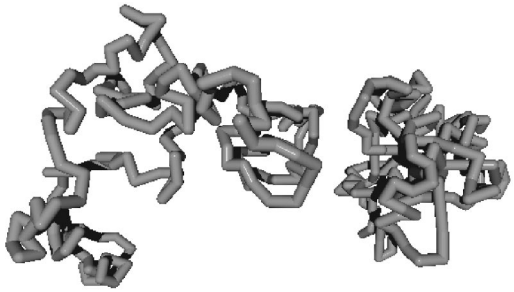

FIG. 2. Snapshots of the equilibrium configurations of an unknot 0_1 (left) and a $C=18$ even twist knot.

dynamics. It is clear that the latter interaction is of strong topological nature which guarantees that the initial knot will remain of the same type. Different prime knots, mostly of lengths $N=180$ and up to $N=240$, of the torus knots $(3_1,5_1,7_1,\ldots)$, even twist knots $(4_1,6_1,8_1,\ldots)$ and odd twist knots $(3_2,5_2,7_2,\ldots)$ are investigated. We have measured the equilibrium average contour length of these prime knots, they are all of the same length as the linear free chain within 0.8% indicating that the knots are far away from the tight knot limit. Initial configurations, like those shown in Fig. 1 are prepared manually. The knot is then well equilibrated by Monte Carlo moves for a long time, typically ten times the equilibrium relaxation time, then ensemble averages are taken for another extended period, typical by ten times the equilibration time.

III. RESULTS ON THE EQUILIBRIUM DYNAMICS

The dynamics in thermal equilibrium for the torus knot, even twist knot and odd twist knot groups are monitored. Some of the diagrams of these knots are depicted in Fig. 1. These initially prepared knot configurations are then well equilibrated. The snapshots of the typical configurations of the circular unknot and the $C=18$ even twist knot are shown in Fig. 2. The knotted polymer is smaller in size as expected. The detailed dynamics are studied by measuring the autocorrelation function and the mean-square displacement of the knot. Characteristic relaxation times and diffusion coefficients are then extracted from these quantities. Emphasis shall be focused on the dependence of the relaxation and the diffusion dynamics on different knot types. All times are measured in units of Monte Carlo steps/monomer (MCS/monomer), 1 MCS/monomer means on average each monomer has attempted to move once.

A. Time autocorrelation functions and equilibrium relaxation times

The equilibrium relaxation behavior is studied through the measurements of the time autocorrelation of some structural properties of the knot, such as the radius of the gyration, which is defined as

$$A_{Rg}(t)=\frac{\langle R_g(t)R_g(0)\rangle-\langle Rg\rangle^2}{\langle R_g^2\rangle-\langle R_g\rangle^2}, \qquad (1)$$

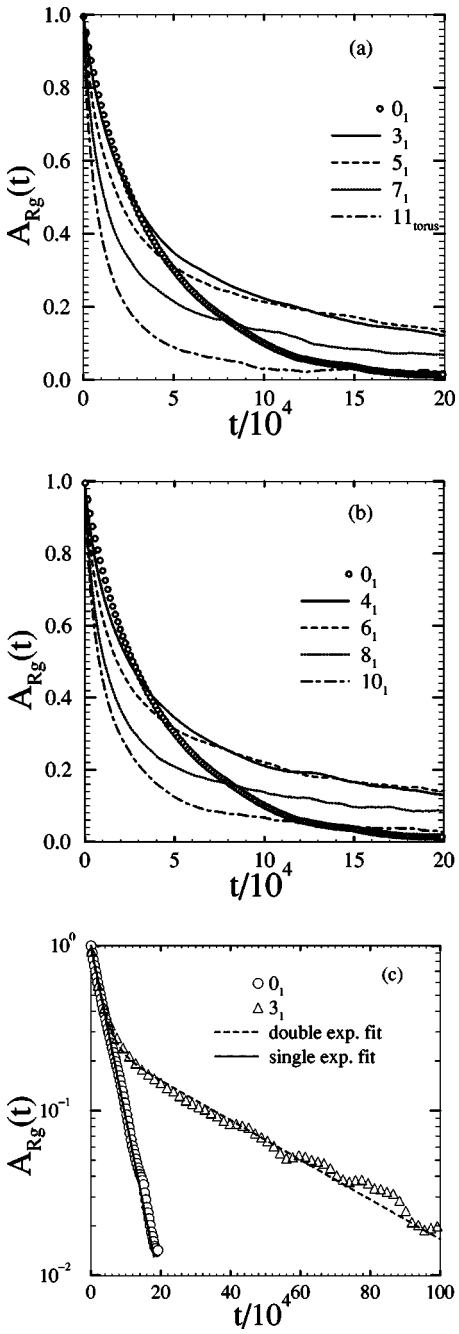

FIG. 3. Time autocorrelation functions for the radius of gyration of various prime knots with $N=180$. t is in units of MCS/monomer. (a) A_{Rg} for the torus knots $3_1,5_1,\ldots$; (b) same as (a) but for the even twist knots $4_1,6_1,\ldots$; (c) semilog plot of the correlation function $A_{Rg}(t)$ for the unknot 0_1 and trefoil knot 3_1.

where R_g is the radius of gyration of the knot, $\langle\cdots\rangle$ denotes thermal average, and time t is measured in Monte Carlo steps per monomer (MCS/monomer). The typical $A_{Rg}(t)$ for various knots are shown in Figs. 3(a) and 3(b). The correlation function for the unknot 0_1 is also shown for comparison. In general, nontrivial knots with higher values of C decay faster. For nontrivial knots with small values of C (such as 3_1, 4_1), their initial relaxation behaviors are close to that of the unknot, however, all nontrivial knots show a long time

tail in their correlation functions. Such a long-time-scale slow relaxation suggests that topological constraint strongly hinder the relaxation of the nontrivial knots. Furthermore, $A_{Rg}(t)$ in general decays faster for nontrivial knots with more crossings. To examine the relaxation behavior in a more quantitative way, the correlation function is plotted semilogarithmically in Fig. 3(a). The correlation function of the unknot 0_1 can be very well described by a single exponential decay while the other nontrivial knots, such as the trefoil (3_1), as shown, display a rather clear separation of a short time scale decay and a long time scale decay. The $A_{Rg}(t)$ for the nontrivial knots can be fitted quite well by a sum of two exponential decays as

$$A_{Rg}(t) = b\exp(-t/\tau_s) + (1-b)\exp(-t/\tau_\ell), \qquad (2)$$

where τ_s and τ_ℓ are the short and long characteristic relaxation times, respectively, and b is the relative weight of the shorter decay. The separation of two distinct time scales in equilibrium relaxation in knots has also been observed previously by Quake [16] who considered $3_1, 4_1, 6_1, 8_1$, and 10_1 knots by using another polymer model. By fitting $A_{Rg}(t)$'s for different knots of $N=180$, the values of τ_s and τ_ℓ are extracted. For the unknot, the relaxation is almost a single exponential since $b \sim 0.1$ only. For other nontrivial knots, although the relaxation behavior is mostly dominated by the shorter relaxation ($b > 0.5$ in most cases), the relaxation changes appreciably to the longer relaxation at later times. Typically, τ_ℓ is ~ 10–30 times larger than τ_s for nontrivial knots with $C \leqslant 10$.

The faster relaxation time scale can be measured by τ_s, or even more conveniently and accurately by the half-decay time $T_{1/2}$ that is defined as the time needed for A_{Rg} to decay to $\frac{1}{2}$. As illustrated in Fig. 3(c), $T_{1/2}$ lies well within the fast time scale regime and reflects mainly the fast relaxation of the knot. Figure 4(a) displays the half-decay times as a function of C for various prime knots in different groups. All the data fall roughly on the same curve suggesting that the fast relaxation time is mainly determined by the essential crossing number of the knot. However, the detailed topology of the knot still has some observable effect on the relaxation times, since even for knots with the same C the $3_1, 5_1, 7_1$ group always has a slightly larger $T_{1/2}$ than the $5_2, 7_2, 9_2$ group. For $C > 15$, the value of $T_{1/2}$ saturates to some minimal value. Our data for the fast relaxation times do not agree with the theoretical result obtained by Quake [16] which predicted the relaxation time scales as $\sim N^{1+2\nu} C^{2/3-2\nu} \simeq N^{2.2} C^{-0.533}$. Our data agree with the scaling of $N^{1+2\nu}$, as N becomes large, but deviate a lot from the scaling of C. The decrease of $T_{1/2}$ with C is much stronger (as compared with Quake's result) for small values of C and seems to saturate to some constant for larger values of C. Furthermore, this scaling exponent in C was also not satisfactorily verified by the simulation data in Ref. [16] in which knots up to ten crossings were studied and fast relaxation time were fitted with a variation of $\sim C^{-0.7}$. A plausible cause of this discrepancy of the scaling prediciton with the simulation data is further explored in Sec. IV. The longer relaxation times for various knots in three knot groups are plotted as a function of C in Fig. 5(b). τ_ℓ varies somewhat irregularly with C even within a group, especially for a smaller value of C. However, τ_ℓ shows an average decreasing trend with increasing C.

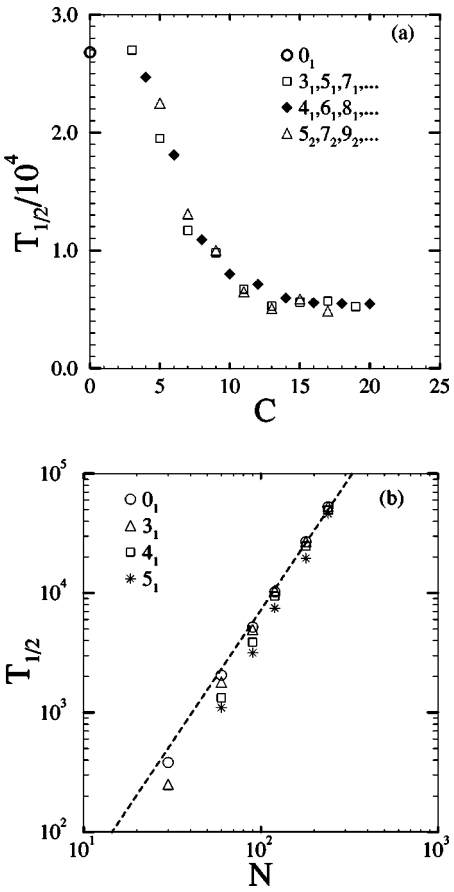

FIG. 4. (a) The half-decay time $T_{1/2}$ of $A_{Rg}(t)$ for various prime knots of lengths $N=180$. (b) Log-log plot of $T_{1/2}$ as a function of the knot length for the unknot and nontrivial knots. The slope of the dashed straight line is $1+2\nu \approx 2.2$.

The nature of these fast and slow relaxation behaviors can be further explored by considering the variations of these relaxation times with the length of the knot. To examine the chain length dependence, the autocorrelation functions of the knots 0_1, 3_1, 4_1, 5_1, 5_2, and 6_1 up to $N=240$ are measured. The values of $T_{1/2}$ and τ_ℓ are then extracted and their variation with N are shown in Fig. 4(b) on a log-log plot. The fast relaxations show a very nice Rouse relaxation behavior with $T_{1/2} \sim N^{1+2\nu}$ for the unknot for $N > 30$. For nontrivial knots, it appears that the finite-N correction to the $N^{1+2\nu}$ becomes more significant for knots with higher C. However, in the large N limit, i.e., when the knots are far from being tight, the values of $T_{1/2}$ for different knots converge to the same value. On the other hand, the slow relaxation times of the nontrivial knots also suggest a power law with $\tau_\ell \sim N^\alpha$, with a knot-type-dependent exponent α. The values of α for these knots are displayed in Table I. The exponent of the slower relaxation time α increases with C in general. Although the exponents α show some dependence on the knot type, their values are only somewhat greater that $1+2\nu \simeq 2.2$ suggests that the overall equilibrium relaxation picture

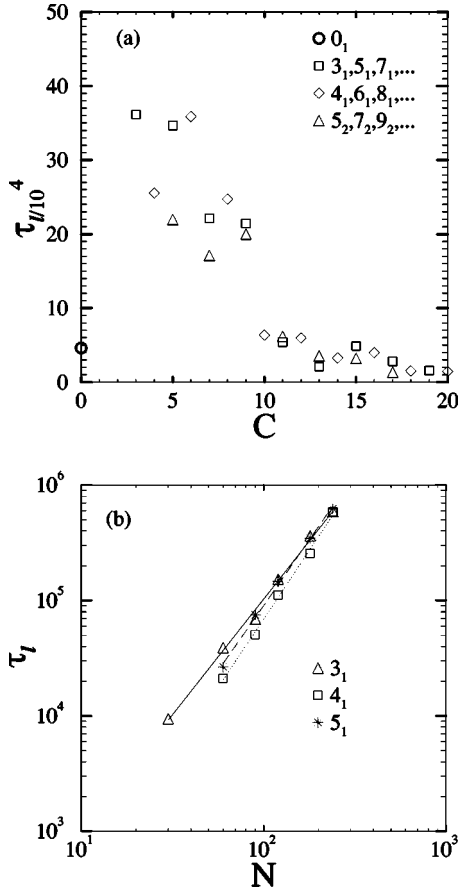

FIG. 5. (a) The slower relaxation times $\tau_{\not/}$, in units of MCS/monomer, as a function of C for various knots. (b) Log-log plot of $\tau_{\not/}$ as a function of the knot lengths. The straight lines are best fits from which the values of the exponent α are obtained.

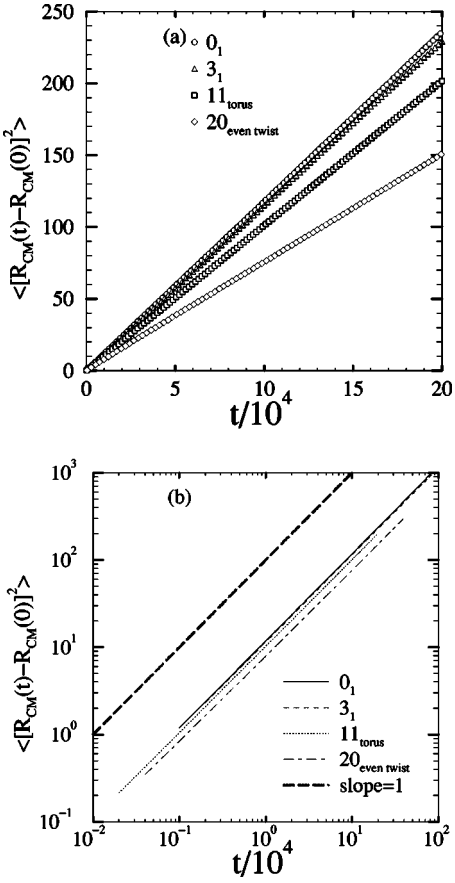

FIG. 6. Mean-square displacement of the center of mass of the knot as a function of time for various knots of lengths $N=180$. t is in units of MCS/monomer. (a) Linear plot. (b) Log-log plot.

of the nontrivial knots can be approximately described by the Rouse model with some corrections. Presumably, such correction originates from the topological constraint of the essential crossings within the nontrivial knot.

The general trend of decreasing of both fast and slow relaxation times with C indicates that more complex knots respond faster. This is due to the fact that more complex knots are in general more compact and exhibit stiffer elastic behavior. The latter properties have also been observed in our recent simulation studies [19] on the deformation of polymer knots.

B. Mean-square displacement and diffusion coefficients

To investigate the diffusion transport dynamics of knotted polymers, the mean-square displacement of the center-of-mass position, $\vec{R}_{cm}$, of the knot is monitored. Figure 6 show the mean-square displacements of different knots as a function of time. The mean-square displacement varies linearly with t indicating a free diffusion behavior for both the unknot and nontrivial knots up to 20 crossings. However, the diffusion is slower for knots with more essential crossings. The self-diffusion coefficient is extracted from the mean-square displacement data as

$$D=\lim_{t\to\infty}\frac{\langle[\vec{R}_{cm}(t)-\vec{R}_{cm}(0)]^2\rangle}{6t} \tag{3}$$

and is plotted against C in Fig. 7(a) for various knots. D shows a general decreasing trend with increasing C and also is not sensitive to the knot types. The diffusion behavior can further be explored by examining the dependence of D on N as shown in Fig. 7(b) for the unknot and some nontrivial knots. The diffusion coefficient of the unknot shows a very nice $1/N$ Rouse behavior, while for the 3_1 and 4_1, such a $1/N$ behavior is also observed for $N>30$. For $N\leqslant 60$, the values of D are smaller, this is due to the fact that when the knot is tight and the local density is higher, the local segment motion of the knot may crossover to some kind of creeping motion in a tube, or quasireptation behavior. However, the values of D for different knots approach the same value in the large N limit, thus the self-diffusion behavior follows the Rouse dynamics for knots in the asymptotic long chain limit.

IV. SCALING ANALYSIS

In this section, we attempt to understand the simulation results in terms of scaling concepts in polymer physics. Since a detailed mathematical description of knots is still at the level of classification, one is still far away from any

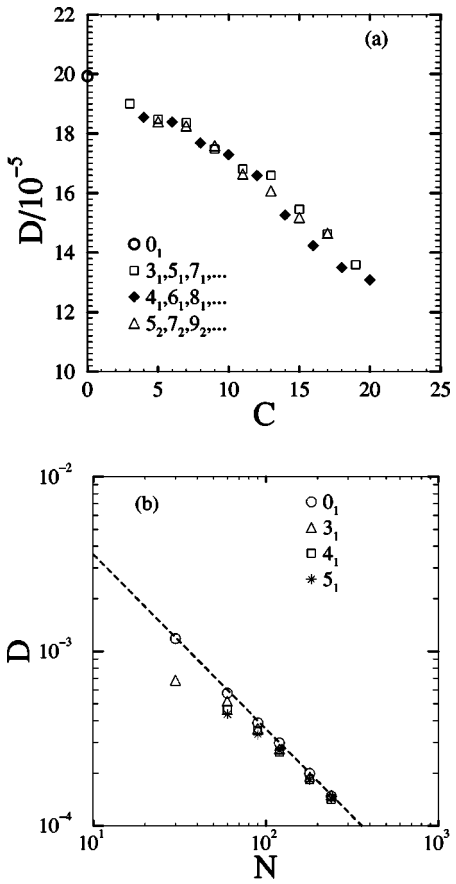

FIG. 7. (a) Diffusion constant D versus C for various knots of lengths $N=180$. (b) Log-log plot of D versus N for the unknot and nontrivial knots. The dashed straight line indicates a slope of -1.

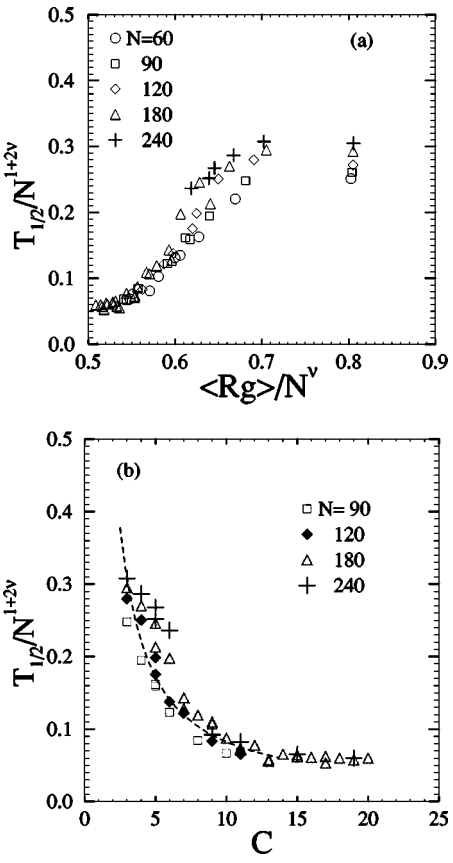

FIG. 8. (a) Scaling plot of $T_{1/2}/N^{1+2\nu}$ versus $\langle R_g\rangle/N^{\nu}$ for the unknot and nontrivial knots. (b) Scaling plot of $T_{1/2}/N^{1+2\nu}$ versus C for nontrivial knots. The dashed curve shows a $1/C^{1.2}$ behavior.

detailed theory on the physical properties of knots and the scaling approach remains to be the most useful theoretical tool at present. Using the blob picture in polymer, which account for the excluded volume interactions among the chain segments, the scaling form for the fast relaxation time is derived under suitable assumptions. Furthermore, the extra monomer-monomer friction in a knotted polymer is taken into account in the maximally inflated tube model and the scaling behavior of diffusion coefficient can be obtained. The value of the self-avoiding walk exponent ν is taken to be $\nu=3/5$ throughout the scaling analysis.

A. Scaling of $T_{1/2}$

Our data, such as in Fig. 4(b) suggest the fast relaxation times scale as $N^{1+2\nu}$ asymptotically. The difference in $T_{1/2}$ for different knot types originates from the different fast elastic response times of the knots. Therefore, we plot in Fig. 8(a) the scaled fast relaxation time of various knots as a function of the mean radius of gyration in units of N^{ν}. The data show a rough scaling behavior suggesting the following scaling form:

$$T_{1/2}=N^{1+2\nu}G(\langle R_g\rangle/R_F), \tag{4}$$

where $R_F\simeq aN^{\nu}$ is the free Flory radius of the polymer under no topological constraint, i.e., a free linear chain and a is the monomer size. G is some scaling function of the strain deformation of the polymer. Thus the above scaling form suggests that the fast relaxation time scale is basically the elastic response of the knot. The extra stiffness of the knotted polymer as compared to the free linear polymer is given by the topological constraint of the formation of a knot, which is in turn predominantly provided by the entanglement effects among the chain segments. Furthermore, the increase in excluded volume interactions in a knot arises fundamentally from the topological constraint of maintaining the knot to be of the same type which forces the polymer to remain strongly entangled. From our data in Fig. 8(a), $G(x)$ is an increasing function, this can be compare with the result of the period of oscillation of a solid elastic sphere [32] that is proportional to the radius of the sphere. For a nontrivial prime knot of N monomers and with C essential crossings, on average the first monomer will be close to the (N/C)th monomer due to the topological constraints and hence can be modeled as a blob of with N/C segments. Exploiting the idea of the blob concept in polymer physics, the length scale of the blob size is $\xi_b\approx(N/C)^{\nu}$. The average number of blobs is C. The relaxation time within a blob scales as $\tau_b\sim(N/C)^{1+2\nu}$ and for $C\gg1$, the relaxation of the whole knot can be viewed as the relaxation of C self-avoiding blobs, thus the time needed for the relaxation to cover a region composed of a random walk of C blobs is

$$T_{1/2} \sim C^{1+2\nu}\tau_b \sim N^{1+2\nu} \approx N^{11/5} \quad \text{for} \quad C \gg 1, \tag{5}$$

which is independent of C. On the other hand, for $C \sim O(1)$ the knot no longer has the configuration of a self-avoiding walk of blobs but rather consists of a small number of blobs that are more or less space filling, then the time needed for the relaxation to propagate through the knot is of the order

$$T_{1/2} \sim C\tau_b \sim N^{1+2\nu}C^{-2\nu} \approx N^{11/5}C^{-6/5} \quad \text{for} \quad C \sim O(1). \tag{6}$$

Again the above two scalings can be summarized in the following scaling form:

$$T_{1/2} = N^{1+2\nu} g(C), \tag{7}$$

where $g(C) \sim$ constant for $C \gg 1$ and $\sim C^{-2\nu}$ for $C \sim O(1)$. The above scaling form is checked by our simulation data and the result is shown in Fig. 8(b) which should be compared with the scaling function $g(C)$ above. For $C > 13$, the data indeed settle to a constant while for smaller values of C, the data for different values of N do fall roughly as $\sim C^{-1.2}$ (dashed curve). There are some scattering in the scaled data, which is due to the correction of finite-N in the exponent in N. It should be noted that the scaling form in Eq. (7) is consistent with the scaling forms in Eqs. (4) and (7); this suggests that $\langle R_g \rangle / N^{\nu} = f(C)$ for some function f that decreases with C and $f(C) \sim$ const for $C \gg 1$. This scaling behavior of $\langle R_g \rangle$ is also observed in our data that will be reported elsewhere [33,34].

B. Maximally inflated knot and scaling of *D*

The relaxation motion of monomers in a knot can be pictured as confined inside an imaginary inflated knotted tube, or the ''ideal form'' [15] of the knot. Grosberg *et al.* [21] introduced a new topological invariant p defined as the aspect ratio of the length (L) to the diameter (d) of a knotted polymer at its maximum inflated state,

$$p = L/d. \tag{8}$$

The diffusion coefficient of the knot can be calculated according to the Einstein relation, $D = k_B T/\mu_t$, where k_B is the Boltzmann's constant and μ_t is the total friction coefficient. In Rouse model [35,36], the friction coefficient is proportional to the number monomers N in the macromolecule, i.e., $N\xi$, where ξ is the monomer-solvent friction coefficient. For a linear polymer chain, the monomers tend to avoid each other in good solvents and the probability of two monomers in direct close contact is small. However, for knotted polymers, monomers are forced to be in close contact because of the topological constraint. During the relaxation process, monomers will slide onto each other, and extra friction results. The collision probability among the monomers is greatly increased as the number of crossings increases. To estimate this extra internal friction, the monomer-monomer friction coefficient is assumed to be proportional to the ratio of length to cross-section area of the maximally inflated knot [17]. Thus the total friction coefficient can be expressed as $\mu_t = N\xi + L\zeta$, where ζ represents the monomer-monomer friction coefficient and $\zeta \simeq \zeta_o/d^2$ for some characteristic monomer-monomer friction ζ_o. Following the idea on the construction of the maximally inflated tube, Grosberg *et al.* obtained $L \sim R_g p^{2/3}$ and $d \sim R_g p^{-1/3} \sim N^{\nu} p^{-3/5}$. Then $\mu_t = N\xi + \zeta_o N^{-\nu} p^{8/5}$ and hence

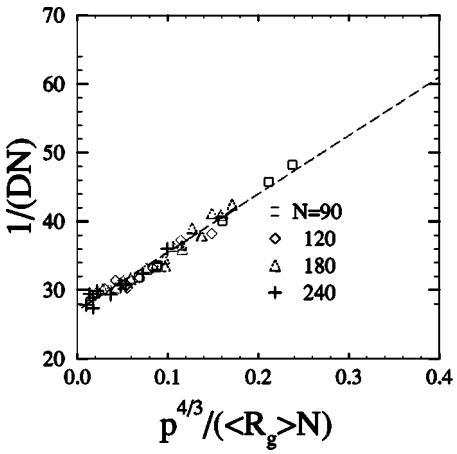

FIG. 9. A plot of $1/(DN)$ versus $p^{4/3}/(\langle R_g \rangle N)$ for various types of knots of different lengths. The dashed curve denotes the linear behavior given in Eq. (9).

$$\frac{k_B T}{D} = N\xi + \frac{p^{4/3}}{R_g}\zeta_o. \tag{9}$$

On average, p varies linearly with C and the values of p for various prime knots in their ideal forms have been calculated in Ref. [4]. By fitting the values of p with C, we obtain $p = 3.78C + 6$ and the values of p for all the knots in this study are then calculated using this linear relation. Figure 9 plots $1/(DN)$ against $p^{4/3}/(\langle R_g \rangle N)$ for various prime knots with different lengths, the data collapse rather well and fall onto a straight line verifying the scaling result in Eq. (9). One recovers the standard Rouse behavior of $D \sim 1/N$ in Eq. (9) for knots with $p \ll N$ (i.e., for knots with smaller values of C) which agrees with the observed behavior in Fig. 7(b). In fact, the relation $T_{1/2} \sim \langle R_g^2 \rangle / D$ does not hold for polymer knots, but was used in Ref. [16] for the derivation of the scaling of the relaxation times and hence lead to the disagreement in the C dependence with the simulation data. In general, $T_{1/2} < \langle R_g^2 \rangle / D$ as indicated by our simulation data. This is because $T_{1/2}$ is the fast relaxation time of the knot that reflects the time scale of global elastic response, while $\langle R_g^2 \rangle / D$ is the time scale originated from the frictional drag experienced by the knot segments, which has a stronger dependence on the detailed topology and hence is in general slower than $T_{1/2}$.

V. DISCUSSIONS AND OUTLOOK

It appears that the decrease in relaxation times with C maybe related to the increase in local density in the interior of the knot. The interior segments in the knot experience a local volume fraction $\phi \propto Na^3/\langle R_g \rangle^3$, and hence ϕ increases with C. For a system with many linear polymers, it is well-known that the relaxation behavior follows the Rouse behav-

ior in the dilute regime for $\phi < \phi^*$, where ϕ^* is the volume fraction for polymer overlapping becomes significant. This cross-over volume fraction scales as $\approx \phi^* \sim N^{1-3\nu}$ and $\phi/\phi^* \sim N^{3\nu} a^3/\langle R_g \rangle^3$. From our data in Fig. 8, the most dense case in our study corresponds to $\phi/\phi^* \sim 0.015$, which is well below the semidilute regime [25]. This suggests that the decrease of the fast relaxation time have little or no contribution from the density effect arising from the screening of pure excluded volume effects. We believe that the dominant reason for the decrease in relaxation times with increasing C in a knot is primarily the increase in the entanglement effects among the segments. For knots with larger C, this entanglement effect is stronger and the knot can be roughly viewed as a cross-linked network (but the crossings are not fixed) and this network becomes stiffer for knots with more essential crossings. The relaxation time reflects the global elastic response time scale of the knot.

It is worth noting that most of the equilibrium physical properties, such as equilibrium sizes [17] and autocorrelation decay times, self-diffusion coefficients. etc., of a knot, vary more or less monotonically with C and could not distinguish different knot groups, with the only exception known so far is the geometrical quantity of the mean writhe number [20]. On the other hand, the equilibrium relaxation time is not very sensitive to the local topological details of the knot and hence different knot types with the same C have close relaxation times. Only by cutting the knot and releasing the strong topological constraints, will such a classification into different knot groups emerge [17,18]. One can imagine that by cutting the knot and relax to the linear free chain, the chain releases some sort of free energy that we call ''topological free energy,'' since its dominant contribution comes from topological interactions. By cutting the knot, the topological free energy is then dissipated by Brownian-type motions in some characteristic nonequilibrium relaxation time scale.

In this paper, we only consider the transport of a single-knotted polymer in good solvents; on the other hand, the transport dynamics of knots in a dense medium will strongly affect the conformation of the knot and thus couple with the topological interactions. Such a situation will occur in experiments of gel electrophoresis of knotted molecules.

ACKNOWLEDGMENTS

This research was supported by the National Council of Science of Taiwan under Grant No. NSC 90-2118-M-008-037. Computing time provided by the Simulational Physics Lab., National Central University is gratefully acknowledged.

[1] W.R. Bauer, F.H.C. Crick, and J.H. White, Sci. Am. **243** (1), 100 (1980).
[2] N.R. Cozzarelli, S.J. Spengler, and A. Stasiak, Cell **42**, 325 (1985).
[3] S.A. Wasserman and N.R. Cozzarelli, Science **232**, 951 (1986).
[4] A. Stasiak, V. Katritch, J. Bednar, D. Michoud, and J. Dubochet, Nature (London) **384**, 122 (1996).
[5] Y. Arai, R. Yasuda, K.-I. Akashi, Y. Harada, H. Miyata, K. Kinoshita, Jr., and H. Itoh, Nature (London) **399**, 446 (1999).
[6] V.V. Rybenkov, C. Ullsperger, A.V. Vologodskii, and N.R. Cozzarelli, Science **277**, 690 (1997).
[7] J. Yan, M.O. Magnasco, and J.F. Marko, Nature (London) **401**, 932 (1999).
[8] V.F.R. Jones, Bull. Am. Math. Soc. **12**, 103 (1985).
[9] F.Y. Wu, Rev. Mod. Phys. **64**, 1099 (1992).
[10] L.H. Kauffman, *Knots and Physics*, 2nd ed. (World Scientific, Singapore, 1993).
[11] *Gauge Fields, Knots and Gravity*, edited by J. Baez and P.J. Muniain (World Scientific, Singapore, 1994).
[12] L. Faddeev and A.J. Niemi, Nature (London) **387**, 58 (1997).
[13] V. Katritch, J. Bednar, D. Michoud, R.G. Scharein, J. Dubochet, and A. Stasiak, Nature (London) **384**, 142 (1996).
[14] V. Katritch, W.K. Olson, P. Pieranski, J. Dubochet, and A. Stasiak, Nature (London) **388**, 148 (1997).
[15] *Ideal Knots*, edited by A. Stasiak, V. Katrich, and L.H. Kauffman (World Scientific, Singapore, 1998).
[16] S.R. Quake, Phys. Rev. Lett. **73**, 3317 (1994).
[17] Y.-J. Sheng, P.-Y. Lai, and H.-K. Tsao, Phys. Rev. E **58**, R1222 (1998); Physica A **281**, 381 (2000).
[18] P.-Y. Lai, Y.-J. Sheng, and H.-K. Tsao, Phys. Rev. Lett. **87**, 175503 (2001).
[19] Y.-J. Sheng, P.-Y. Lai, and H.-K. Tsao, Phys. Rev. E **61**, 2895 (2000).
[20] J.-Y. Huang and P.-Y. Lai, Phys. Rev. E **63**, 021506 (2001).
[21] A.Yu. Grosberg, A. Feigel, and Y. Rabin, Phys. Rev. E **54**, 6618 (1996).
[22] A.Yu. Grosberg, Phys. Rev. Lett. **85**, 3858 (2001).
[23] I. Carmesin and K. Kremer, Macromolecules **21**, 2819 (1988); J. Phys. (Paris) **51**, 915 (1990).
[24] H.-P. Deutsch and K. Binder, J. Chem. Phys. **94**, 2294 (1991).
[25] W. Paul, K. Binder, D.W. Heermann, and K. Kremer, J. Phys. (Paris) **1**, 37 (1991); J. Chem. Phys. **95**, 7726 (1991).
[26] G. Burde and H. Zieschang, *Knots* (Walter de Gruyter, Berlin, 1985).
[27] P.G. Tait, *Scientific Papers* (Cambridge University Press, Cambridge, England, 1898), Vol. I, p. 273.
[28] C.N. Little, Trans. Conn. Acad. Arts Sci. **18**, 374 (1885).
[29] J.W. Alexander and G.B. Briggs, Ann. Math. **28**, 562 (1926).
[30] J.H. Conway, in *Computational Problems in Abstract Algebra*, edited by J. Leech (Pergamon, New York, 1970).
[31] K. Kremer and G.S. Grest, in *Monte Carlo and Molecular Dynamics Simulations in Polymer Science*, edited by K. Binder (Oxford University Press, New York, 1995).
[32] L.D. Landau and E.M. Lifshitz, *Theory of Elasticity*, 3rd ed. (Pergamon Press, New York, 1986).
[33] P.-Y. Lai, Chin. J. Phys. **40**, 107 (2002).
[34] P.-Y. Lai, Y.-J. Sheng, and H.-K. Tsao (unpublished).
[35] P.G. de Gennes, *Scaling Concepts in Polymer Physics* (Cornell University Press, Ithaca, NY, 1979).
[36] M. Doi and S.F. Edwards, *The Theory of Polymer Dynamics* (Oxford University Press, Oxford, 1992).